Plasma Jets from Laser-Irradiated Planar Targets

E. F. Gabl, B. H. Failor, C. J. Armentrout, N. D. Delamater, W. B. Fechner, R. A. Bosch, Gar E. Busch, and Z. M. Koenig
KMS Industries, 700 KMS Place, Ann Arbor, Michigan 48106

D. Ress and L. Suter
Lawrence Livermore National Laboratory, Livermore, California 94550

R. J. Schroeder
Schlumberger-Doll Research, Old Quarry Road, Ridgefield, Connecticut 06877-4108
(Received 21 June 1989)

We have observed plasma jets from laser-irradiated gold disk targets. The structures originate from low-intensity regions of the incident laser beam but propagate much faster than similar density surfaces from higher-intensity regions. The material is both cold and dense, as evidenced by its emission of soft x rays and absorption of hard x rays.

PACS numbers: 52.40.Nk, 52.40.−w

Jets and irregular structures have been observed in laser-produced plasmas for a number of experiments. The structures occur under a variety of experimental conditions and have been measured with several diagnostics. Stamper and Ripin[1] and Stamper, McLean, and Ripin[2] used a 0.53-μm probe to make Faraday-rotation measurements on low-Z targets illuminated by a 1.06-μm laser with intensity from 10^{15} to 10^{16} W/cm^2 for 100 ps. Fine-scale structure in the field was observed. Fine-scale jets were seen in Faraday-rotation measurements made by Grek *et al.*[3] Low-Z targets were irradiated by a CO_2 laser with intensity of 10^{14} W/cm^2 in a 1.4–1.7-ns pulse. The jets originate from densities up to 16 times critical and were observed during the laser pulse. Thiell and Meyer[4] show shadowgrams of jetlike structures emerging from both sides of Al or Au thin-foil targets. The laser was either 1.06 or 0.351 μm in an 850-ps pulse with irradiance from 10^{13} to 5×10^{14} W/cm^2. Small-scale jets were present from 2 to 7 ns after the peak of the laser pulse. The characteristics of the structures observed in the experiments described above can be summarized as (1) filamentary as opposed to billowing; (2) more pronounced for higher Z, higher intensity, and longer wavelength; (3) associated with strong azimuthal magnetic fields; and (4) appearing after the laser has shut off (except for the CO_2 illumination). Thermoelectric[5] and radiative cooling[6] instabilities have been invoked to explain these phenomena. The observed jets have been associated with high-intensity "hot" spots in the incident laser beam.

In this Letter we present data that show jets and filamentary structures issuing from low-intensity "cold" spots in the incident beam. The jet is cold relative to the coronal plasma, has a mass density much higher than that of the background corona, and moves faster than material of similar density in the coronal plasma. We have attempted to generate coronal jets with 2D hydrodynamic simulations, but have not been successful; the jetting phenomena is apparently not purely hydrodynamic.

Gold disk targets (22 μm thick, 600 μm in diameter) were irradiated using the CHROMA laser at $\lambda=0.5265$ μm. For 0.351-μm illumination, the results are qualitatively similar. The incident laser intensity was from (1 to 5)$\times10^{14}$ W/cm^2. The spot diameter was either 200 or 500 μm, obtained by placing the target 1200 or 3000 μm from the best focus of an $f/6$ aspherical lens. The laser pulse shape was varied by stacking up to thirteen individual variable-amplitude pulses, each 125-ps full width half maximum, spaced by 170 ps. 1-ns pulses were formed from six stacker pulses. Three picket pulses were formed by stacking pulses 1, 6, and 8–13 in the approximate amplitude ratios 1:2:3 (Fig. 1). The measured absorption was (75–85)%. The jetting was observed with three diagnostics. A time-integrated Kirkpatrick-Baez (KB) microscope (resolution better than 7 μm) imaged soft x rays (600–800 eV) orthogonal to the laser axis. A secondary image is present in the data shown but offset from the region of interest. Pinhole cameras (resolution better than 10 μm) imaged the time-integrated M-band

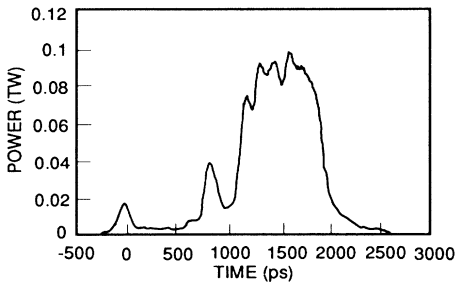

FIG. 1. From 100 to 150 J were used in a 2-ns picket laser pulse obtained by stacking 125-ps pulses.

emission (2–4 keV) perpendicular and parallel to the laser direction. Holographic interferograms[7] were taken with up to four frames (400-ps spacing) per shot. The probe beam had wavelength $\lambda = 0.265$ μm and was 20 ps in duration.

The phenomena were observed for both 1200- and 3000-μm focal offsets. Two cases of target position relative to the best focus will be discussed. For divergent focus, random modulations of the Gaussian intensity pattern are seen in spikes of width 20 to 50 μm with a peak-to-valley intensity from 2 to 4. On the convergent side of best focus is a high-intensity ring with peak intensity from 3 to 6 times that at the center. The ring width is from 25 to 50 μm, and the diameter is either 100 or 250 μm for 1200- and 3000-μm focal offset, respectively. The equivalent target-plane images on both sides of focus showed similar inhomogeneities regardless of temporal pulse shape. The large-scale intensity profile is also apparent in the M-band emission from the front of the target. For convergent focus, the peak emission is from 2 to 5 times higher than the emission in the center of the ring. For divergent focus, the smaller-scale fluctuations are smoothed out, but the overall spot size is the same as that obtained from the equivalent plane image.

The most dramatic evidence of plasma jets can be seen with the target placed 1200 μm on the convergent side of best focus. Figure 2 shows several data for a target illuminated with a picket-fence pulse with peak intensity of 5×10^{14} W/cm^2. Interferograms [Figs. 2(a)–2(d)] were taken at 320, 720, 1120, and 1520 ps relative to the beginning of the laser pulse. Visible in the second frame is a jet 20–30 μm wide at the outermost fringe. By the third frame this jet extends 370 μm from the target. Using the location of the fringes, we estimate the velocity to be 5×10^7 cm/s between frames two and three. Assuming cylindrical symmetry of the jet and a parabolic profile, the electron density of the jet is about 6×10^{20}/cm^3. Abel inversion of the interferogram, not including the jet, yields a coronal density less than 2×10^{19}/cm^3. The jet expands 4 times faster than that portion of the background corona profile at a similar density. By the fourth frame, the second and third pickets have arrived and the jet is smoothed out. The pinhole picture [Fig. 2(e)] taken perpendicular to the laser beam shows a region of low emission extending 125 μm from the target surface. Film scans show that the jet is 120 μm wide at its base and narrows to 15 μm near its apex. The region of low M-band emission correlates well with the region of high soft-x-ray emission measured by the KB microscope [Fig. 2(f)]. This region extends from 60 to 130 μm from the target surface and is from 90 to 30 μm wide. We do not expect to see the soft-x-ray emission from the jet near the target surface since the plasma there is optically thick.

The interferometric and x-ray pictures can be explained if the jets are cold relative to the corona. If the

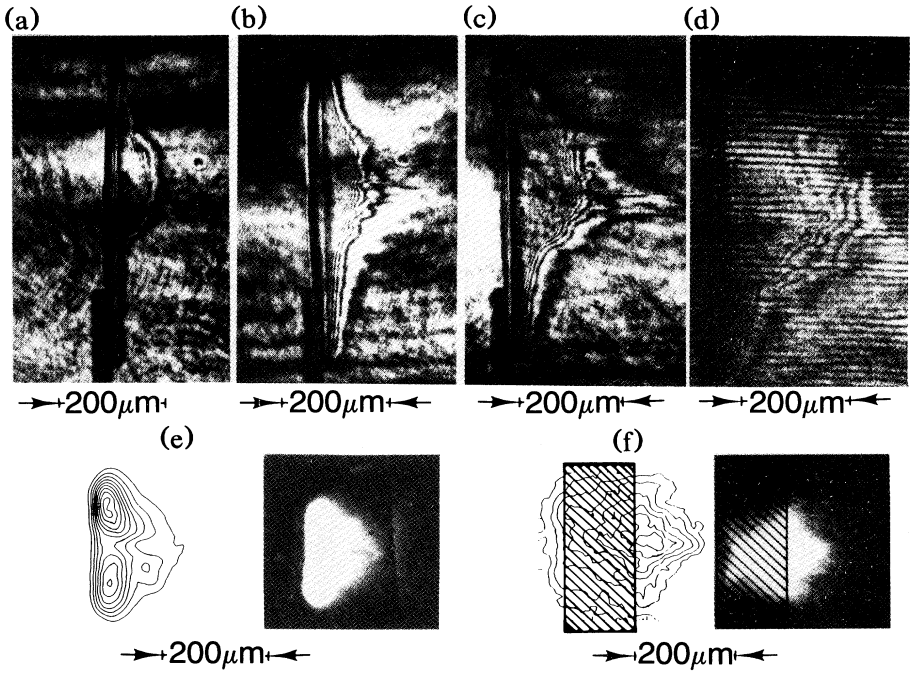

FIG. 2. Jetting is observed with a 1200-μm offset on the convergent side of best focus for a 2-ps picket laser pulse. Interferograms taken at (a) 320, (b) 720, (c) 1120, and (d) 1520 ps show the evolution of the jet. (e) The M-band x-ray image and (f) the soft-x-ray image indicate that the jet is cool.

jets were hot initially, or heated by thermal conduction from the corona, we would expect the jet to thermalize and expand uniformly into the background plasma. (This appears to occur during the second and third pickets, when energy is continuously being absorbed by the target.) Since the jetted material radiates more in the low energies and less in the high energies, we conclude that the jets are colder than the background corona.

We can use the relative intensities of the x-ray pictures to estimate the mass density of the jet. The M-band emission of the corona backlights the jet. The low intensity of M-band emission on axis suggests that the jet absorbs M-band emission. We assume that the jet is cylindrical, its emission in the M band is negligible, and the surrounding hot corona is cylindrical and optically thin to its own radiation. Using an average opacity of cold gold of 2000 cm^2/g, we obtain a lower bound of the average mass density of about 0.02 g/cm^3, 50 μm from the target surface, and 0.09 g/cm^3, 100 μm from the target surface. This is $\frac{1}{1000}$ to $\frac{5}{1000}$ of the solid mass density. This is consistent with the electron densities found at the outermost fringe.

Finer-scale jets are observed with the target placed 3000 μm on the divergent side of best focus. Interferograms for a picket pulse with peak intensity 1×10^{14} W/cm^2 are shown in Fig. 3. In Figs. 3(a) and 3(b) jets 20–30 μm wide issue from the target with a velocity of 5×10^7 cm/s and density $5\times10^{20}/cm^3$. These jets move at an angle away from the laser spot. When the third and fourth pickets arrive, the jets smooth out as for the convergent focus. X-ray pictures show jets corresponding to the features observed in the interferograms. In the x-ray pinhole image [Fig. 3(c)] we see irregularities in the emission near the target surface—presumably corresponding to cold spots. These jets are not identifiable farther than 25 μm from the target surface. The KB microscope shows jets emitting more in the softer-x-ray region and extending out about 100 μm from the target surface [Fig. 3(d)], as observed for convergent focus. Jets were observed by the x-ray cameras only when two picket pulses were used. When the third pulse was present, the x-ray emission from the jets was dominated by emission from the corona. Since these jets were thinner and perhaps more tenuous than for shots with convergent focus, they would be heated faster when the main picket arrived, and would tend to absorb less in the M band and emit less in the soft-x-ray band.

The plasma jets were observed for every shot with 125-ps picket pulses, and with either 1200- or 3000-μm offset. For square 1-ns pulse shots with convergent focus, the fringes from the interferograms showed a smooth distortion–not the spikiness observed for the picket pulses. X-ray pictures showed features corresponding to the hot ring, but these did not extend out from the target as for the picket pulse. This can be interpreted in the same way as the smoothing of the jets observed for picket pulses. Since the laser is on continuously, energy is deposited into the jet by radiation and thermal conduction, smoothing the jet before it propagates through the corona.

Low-Z targets, CH, Al, and Ti, were also shot. Jets were observed with interferometry to varying degrees in each of these elements, decreasing in extent as Z is decreased. Since thermal transport is more efficient in low-Z targets and the radiation losses are lower, keeping the corona hot, jets that are formed could be expected to thermalize faster than those for high-Z targets. Pinhole pictures of the front surface of the target show a more

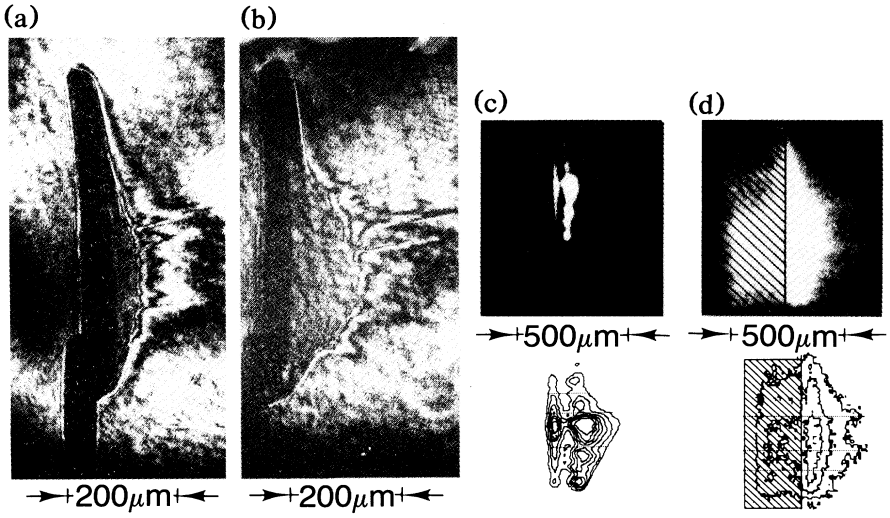

FIG. 3. Jetting is observed with a 3000-μm offset on the divergent side of best focus for a picket laser pulse. Interferograms taken at (a) 320 and (b) 720 ps show a number of small jets. (c) The M-band and (d) soft-x-ray emission indicates that the jets are cool.

homogeneous emission pattern, also evidence of increased smoothing.

In the hydrocode simulations, we tried to seed coronal-jet formation in gold by using a 100-ps laser pulse with a hot annular ring between 100- and 200-μm radius surrounding a cold center of 100-μm radius. The intensity ratio in the laser beam varied from 3:1 to 10:1 for the hot and cold spots. This was an attempt to simulate the convergent-focus shots which experimentally showed the largest size jets for picket pulses.

A possible hydrodynamic explanation for our observations is that a dense column of cold plasma protruding out along the axis might be achieved if laser-beam refraction and absorption begin to "pinch" out the cold material like toothpaste out of a tube, with convergent pressure gradients in the ablation region above critical density. The cold jets would presumably not expand much laterally, due to confinement by the outer ring of hot plasma. The coronal jets, however, never really formed in our simulations. Initially, the isodensity contours bow out farthest in regions of high laser intensity, due to the higher ablation rate there. The higher ablation rate in the high-intensity region caused coronal material in the hot ring to rapidly decouple from slower ablating material in the cooler central region. The two behaved as if they were independently driven. The relative expansion of the hot and cold plasmas is the opposite of what is observed experimentally. Apparently, pure hydrodynamics is not enough to produce the jets. This suggests that the jets may instead be the result of an instability. We examine elsewhere[8] the possible role of the radiative cooling instability and instabilities caused by magnetic field effects. On a more positive note the simulations do show that thermal conduction in gold is inefficient in smoothing out temperature-variation characteristics of cold jets in the free-expansion phase after the first picket pulse.

The implications of plasma jets are greatest for indirect-drive fusion. High-density plasma racing ahead of thermal expansion may move into the laser beam. Laser-light absorption and refraction could result in drive nonuniformity. Additionally, the lateral expansion of the jet could contribute to the formation of long-scale-length plasmas which can lower the threshold of parametric instabilities such as stimulated Raman scattering. The small-scale jets arising from spot nonuniformities could be removed by one of the many beam-smoothing techniques under consideration recently.[9] Larger-scale nonuniformities may present a more significant problem which can be mitigated only by increasing the number of laser spots to improve large-scale uniformity.

This work was prepared for the Department of Energy under Contract No. DE-AC03-87DP10560.

[1]J. A. Stamper and B. H. Ripin, Phys. Rev. Lett. **34**, 138 (1975).

[2]J. A. Stamper, E. A. McLean, and B. H. Ripin, Phys. Rev. Lett. **40**, 1177 (1978).

[3]B. Grek, F. Martin, T. W. Johnston, H. Pepin, G. Mitchel, and F. Rheault, Phys. Rev. Lett. **41**, 1811 (1978).

[4]G. Thiell and B. Meyer, Laser Part. Beams **3**, 51 (1985).

[5]M. G. Haines, Phys. Rev. Lett. **13**, 917 (1981).

[6]R. G. Evans, in *Radiative Properties of Hot Dense Matter,* Proceedings of the Second International Conference on Radiative Processes of Hot Dense Matter, Sarasota, Florida, 1983, edited by J. Davis *et al.* (World Scientific, Singapore, 1985), p. 73.

[7]Gar. E. Busch, C. L. Shepard, L. D. Siebert, and J. A. Tarvin, Rev. Sci. Instrum. **56**, 879 (1985).

[8]N. D. Delamater and W. B. Fechner (to be published).

[9]N. K. Moncur, Appl. Opt. **16**, 1449 (1977); R. Lehmberg and S. P. Obenschain, Opt. Commun. **46**, 27 (1983); Y. Kato *et al.*, Phys. Rev. Lett. **53**, 1057 (1984); University of Rochester Laboratory for Laser Energetics Review **40**, October–December 1988.

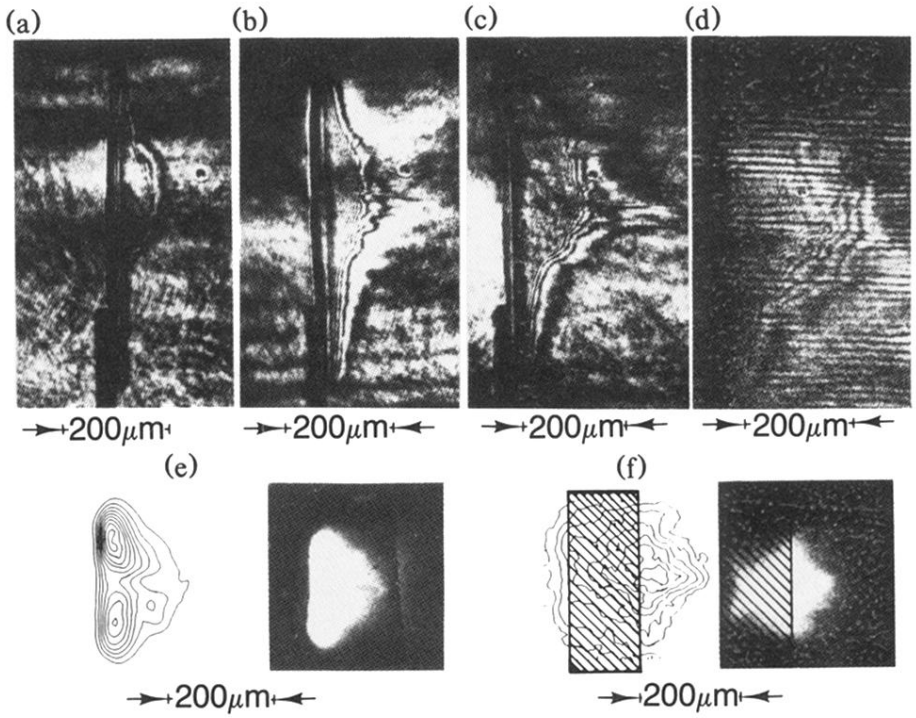

FIG. 2. Jetting is observed with a 1200-μm offset on the convergent side of best focus for a 2-ps picket laser pulse. Interferograms taken at (a) 320, (b) 720, (c) 1120, and (d) 1520 ps show the evolution of the jet. (e) The M-band x-ray image and (f) the soft-x-ray image indicate that the jet is cool.

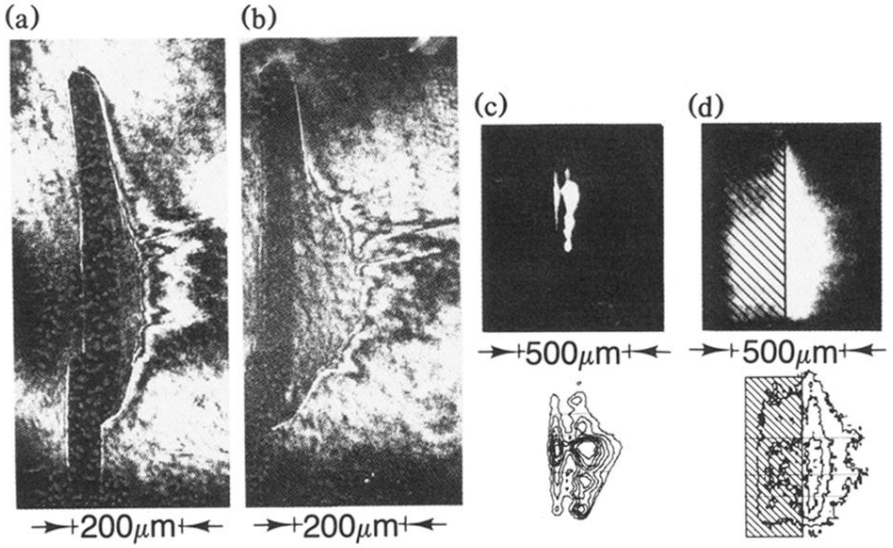

FIG. 3. Jetting is observed with a 3000-μm offset on the divergent side of best focus for a picket laser pulse. Interferograms taken at (a) 320 and (b) 720 ps show a number of small jets. (c) The M-band and (d) soft-x-ray emission indicates that the jets are cool.